Thermal conductivity of thick meso-porous silicon layers by micro-Raman scattering

V. Lysenko,[a)] S. Perichon, B. Remaki, and D. Barbier
Laboratoire de Physique de la Matière, UMR 5511 CNRS, INSA de Lyon, 20 avenue Albert Einstein, 69621 Villeurbanne Cedex, France

B. Champagnon
Laboratoire de Physico-Chimie des Matériaux Luminescents, UMR 5620 CNRS, Université Lyon 1, 69622 Villeurbanne, France

We report here a theoretical model describing specific mechanisms of heat transport in as-prepared and oxidized meso-porous silicon layers. The model is in good agreement with experimental measurements performed by micro-Raman scattering on the layers surface. For the first time, thermal conductivity inhomogeneity along the porous layer thickness of 100 μm is studied. Direct correlation between the thermal conductivity and morphology variations along the layer thickness is brought to the fore. A new approach to estimate local porosity of the porous layers based on thermal conductivity and Si nanocrystallite size measurements is also proposed. © 1999 American Institute of Physics. [S0021-8979(99)08124-4]

I. INTRODUCTION

Porous silicon (PS) whose low thermal conductivity (TC) (two or three order lower then TC of monocrystalline Si) has recently been pointed out[1–6] appears to be a new thermal insulating substrate for microsensor design.[7–9] As it has been observed in our previous work,[9] thick PS layers ($\geq$100 μm) are needed to ensure efficient thermal isolation. Moreover, thick PS layers obtained on heavily doped *p*-type Si (meso-PS) considerably better withstand Complementary metal–oxide–semiconductor (CMOS) procedures usually used for microsensor fabrication than those formed on lightly doped *p*-type Si (nano-PS). Therefore, meso-PS is preferred to be used as new thermal insulating material.

To ensure reproducible high performance of future thermal microsensors, TC of meso-PS has to be well controlled. However, no systematic study describing the influence of fabrication conditions on TC values of meso-PS has yet been performed. In addition, being strongly dependent on preparation conditions and post-fabrication treatments, TC values of meso-PS given in literature[1–4] present considerable differences. Drost *et al.*[1] obtained a relatively high TC value of as-prepared meso-PS layers (80 W m^{-1} K^{-1}), which decreased drastically (down to 2.7 m^{-1} K^{-1}) after 1 h low temperature (300 °C) oxidation in dry O_2 atmosphere. Gesele *et al.*[2] compared TC dependence on temperature of meso- and nano-PS layers with given porosity, thickness, and crystallite size. The authors have also proposed a simple model for heat conduction in PS based on phonon diffusion mechanism. Benedetto *et al.*[3] measured TC of two meso-PS layers with different porosity and thickness (see Table I). In one of our previous work,[6] we proposed a theoretical approach to put in agreement all data obtained earlier[1–3] and to study the influence of thermal oxidation on the TC values. Our model

predicting dynamics of TC evolution along with oxidized fraction of meso-PS was qualitatively illustrated by series of photoacoustic measurements.

In this article, we present a detailed theoretical and experimental TC study of as-prepared and partially oxidized thick (100 μm) meso-PS layers. A theoretical model describing the influence of morphology particularities and thermal oxidation of meso-PS layers on their TC values is proposed. The model is found to be in good agreement with experimental TC measurements performed by means of recently described measurement technique[10] based on micro-Raman scattering. We compare our experimental results with those obtained by other authors and performed by means of thin films microdevices[1,2] and photoacoustic spectroscopy.[3] Based on the theoretical model and simultaneous measurements of TC and characteristic mean size of Si nanocrystallites constituting meso-PS layers,[11–14] a new approach to estimate local layer porosity is proposed. In relation to all TC measurements carried out earlier in relatively thin meso-PS layers,[1–4] we have studied TC inhomogeneity along the meso-PS layer thickness of 100 μm.

II. THEORETICAL MODEL

A. TC of as-prepared meso-PS

Meso-PS layers formed on highly doped *p*-type Si wafers (electrical resistivity of about 0.01 Ω cm) exhibit a clear column structure.[15,16] The layers consist of many long main pores running perpendicularly to the wafer surface and having small side branches. Therefore, a meso-PS layer can be presented as a relatively regular column arrangement of quasispherical Si nanocrystallites [Fig. 1(a)]. According to cross-sectional transmission electron micrographs of meso-PS,[15,16] our model is not far from reality.

As was already described in detail,[6] TC of a meso-PS layer can be defined as

---
[a)]Electronic mail: lysenko@insa-lyon.fr

TABLE I. Room temperature TC and morphology parameters of meso-PS.

| Reference | Original Si wafer | Formation conditions | | PS layer thickness (μm) | Si nano-crystallites size (nm) | TC of as-prepared PS (W m^{-1} K^{-1}) | Porosity (%) |
		Current density (mA/cm^2)	HF concentration (%)				
2	p^+ type, (100)	...	...	21	9.0	0.8	64[a]
3	p^+ type, (111)	15	12	10	...	3.9	50[b]
		15	20	23	...	2.5	60[b]
Our current work	p^+ type, (100)	20	25	100	8.3	4.6	38[c]
		75			7.2	0.9	62[c]
		150			7.0	0.3	74[c]

[a]Measured by gravimetric method.
[b]Measured by reflectivity method.
[c]Calculated from Eq. (5), using experimental TC and Si nanocrystallite size values.

$$k_{\text{meso-PS}} = k_{\text{col}}^{\text{eff}}(1-P)g_0, \tag{1}$$

where P is the layer porosity, g_0 is so-called percolation strength introduced here in the same way as proposed by Gesele *et al.*[2] where the fixed relation between g_0 and the porosity was given:

$$g_0 = (1-P)^2. \tag{2}$$

$k_{\text{col}}^{\text{eff}}$ represents the mean effective TC of Si nanocrystallites constituting the columns. In the case when characteristic mean size of the nanocrystallites (r_{cr}) is less than phonon mean free path in monocrystalline Si at room temperature ($\Lambda_{\text{Si}} = 43$ nm),[17] heat transport in a single nanocrystallite cannot be described by classic Fourier heat conduction theory, where r_{cr} should be much larger than Λ_{Si}. When $r_{\text{cr}} < \Lambda_{\text{Si}}$, there is no phonon scattering inside the crystallites and consequently neither temperature gradient nor the notions of temperature and thermal conductivity can be defined. Phonons scatter only at the crystallite boundaries, which restore local thermodynamic equilibrium. Therefore, only at the boundaries, which act as artificial scatter sites, the notion of temperature can be introduced. Between two opposite boundaries the phonon transport has a ballistic nature. In spite of this, a notion of effective TC of the Si nanocrystal-lites, $k_{\text{col}}^{\text{eff}}$, can be introduced, considering that the phonons scatter at an effective length, Λ_{eff}:[17,18]

$$\Lambda_{\text{eff}} = \frac{\Lambda_{\text{Si}}}{1 + \frac{4}{3}\frac{\Lambda_{\text{Si}}}{r_{\text{cr}}}}. \tag{3}$$
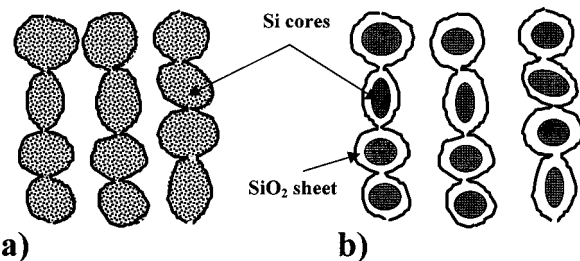

a)   **b)**

FIG. 1. Schematic of the columnar structure of meso-PS: (a) nonoxidized columns, (b) partially oxidized columns.

Therefore, $k_{\text{col}}^{\text{eff}}$ can be determined as

$$k_{\text{col}}^{\text{eff}} = \frac{1}{3}c\nu\Lambda_{\text{eff}} = \frac{k_{\text{Si}}}{1 + \frac{4}{3}\frac{\Lambda_{\text{Si}}}{r_{\text{cr}}}}, \tag{4}$$

where c is the specific heat per unit volume of the Si nanoc-rystallites, ν is the average speed of sound, and k_{Si} is the TC of monocrystalline Si. Inserting g_0 and $k_{\text{col}}^{\text{eff}}$ from Eqs. (2) and (4) into Eq. (1), we obtain

$$k_{\text{meso-PS}} = \frac{k_{\text{Si}}}{1 + \frac{4}{3}\frac{\Lambda_{\text{Si}}}{r_{\text{cr}}}}(1-P)^3. \tag{5}$$

Referring to Eq. (5), TC of as-prepared meso-PS layers ($k_{\text{meso-PS}}$) depends strongly on two main morphological parameters of the layers—porosity (P) and mean size of the Si nanocrystallites (r_{cr}).

B. TC of oxidized meso-PS

After partial oxidation, silicon crystallites of each column are covered with a SiO$_2$ sheet and their initial sizes are reduced [Fig. 1(b)]. In this case, TC of the remained Si cores of the partially oxidized Si/SiO$_2$ crystallites, k_{Si}^*, can be expressed by analogy with Eq. (4) as following:

$$k_{\text{Si}}^* = \frac{k_{\text{Si}}}{1 + \frac{4}{3}\frac{\Lambda_{\text{Si}}}{r_{\text{cr}}\sqrt[3]{(1-\xi)}}}, \tag{6}$$

where $r_{\text{cr}}\sqrt[3]{(1-\xi)}$ represents a new reduced mean size of the remained Si cores and ξ is the oxidized fraction of the Si nanocrystallites defined as

$$\xi = \frac{(V_0^* - V_{\text{Si}}^*)}{2.27V_0}, \tag{7}$$

where coefficient 2.27 considers expansion of the crystallite volume during oxidation, V_0 is the initial volume of the non-oxidized Si crystallite, V_0^* is the total volume of the crystal-lite after the partial oxidation and V_{Si}^* is the volume of the remained Si core of the partially oxidized crystallite.

J. Appl. Phys., Vol. 86, No. 12, 15 December 1999
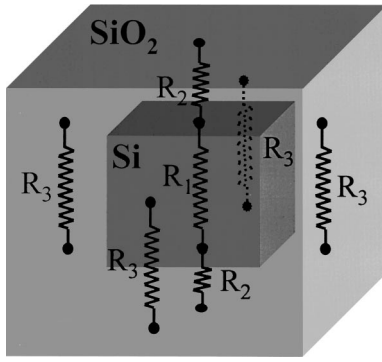
Lysenko *et al.* 6843

FIG. 2. Schematic of a single partially oxidized Si nanocrystallite in cubic form. R_1 is the thermal resistance of the Si core, R_2 are the SiO_2 thermal resistances underneath and above the Si core, R_3 are the SiO_2 thermal resistances around the Si core.

FIG. 3. Validity limit of the theoretical model describing the dependence of the TC on oxidized fraction of the meso-PS layers.

To calculate the TC of a partially oxidized column, we have presented each Si/SiO_2 crystallite in a cubic form (Fig. 2) with a total volume equal to V_0^* of the real quasi-spherical crystallite. Assuming that all crystallites in columns are statistically the same and that each partially oxidized crystallite can be presented as a set of thermal resistances (Fig. 2), TC of partially oxidized columns was found:

$$k_{col}^* = \cfrac{1}{\cfrac{A^{1/3}-B^{1/3}}{k_{SiO_2}A^{1/3}} + \cfrac{A^{1/3}B^{1/3}}{k_{SiO_2}(A^{2/3}-B^{2/3})+k_{Si}^*B^{2/3}}}, \quad (8)$$

where $A=(1+2.27\xi)$, $B=(1-\xi)$ and k_{SiO_2} is the TC of silicon dioxide.

The total TC of the partially oxidized meso-PS layer, $k_{meso-PS}^*$, is defined by analogy with Eq. (1):

$$k_{meso-PS}^* = k_{col}^*(1-P^*)g_0^*, \quad (9)$$

where P^* is the porosity of the oxidized meso-PS layer and g_0^* is its percolation strength defined by analogy with Eq. (2): $g_0^*=(1-P^*)^2$. Assuming that the oxidation process does not change the overall layer volume, P^* can be expressed as the function of initial porosity, P, of as-prepared meso-PS:

$$P^* = 1-(1-P)(1+1.27\xi). \quad (10)$$

Inserting Eq. (6) into Eq. (8) and then Eqs. (8) and (10) into Eq. (9), we obtain

$$k_{meso-PS}^* = \cfrac{(1-P)^3A^3}{\cfrac{A^{1/3}-B^{1/3}}{k_{SiO_2}A^{1/3}} + \cfrac{A^{1/3}B^{1/3}}{k_{SiO_2}(A^{2/3}-B^{2/3})+\cfrac{k_{Si}B^{2/3}}{\left(1+\cfrac{4\Lambda_{Si}}{3r_{Si}B^{1/3}}\right)}}}. \quad (11)$$

This theoretical model can only be applied when pores of the porous layer are not completely filled with the grown silicon dioxide, i.e., in other words when $P^*>0$. The case when $P^*<0$ corresponds to the oxide densification accompanied by a growth of the PS layer volume. Consequently, this case can not be described by our model because the
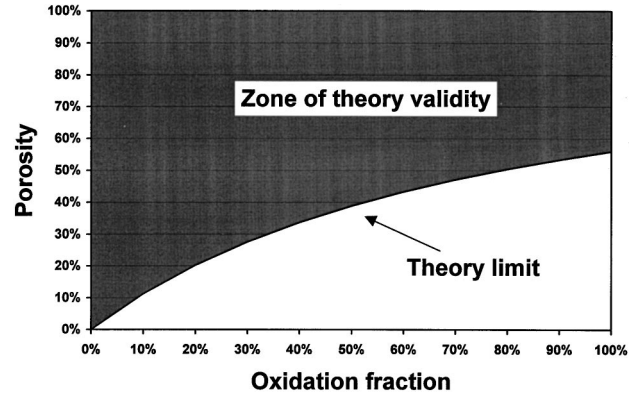
oxide densification dynamics of the meso-PS is unknown. Therefore, the condition $P^*=0$ expresses the model validity limit presented graphically in $P-\xi$ coordinates in Fig. 3. For 56% porosity of as-prepared PS (P), when all Si nanocrystallites are completely oxidized ($\xi=100\%$), the pores are completely filled with SiO_2($P^*=0$), i.e., initial as-prepared meso-PS layer is completely transformed into a single block of SiO_2. For $P>56\%$, when $\xi=100\%$, we obtain $P^*>0$, i.e., it is the case of porous silicon dioxide. For $P<56\%$, our model is only valid for those ξ values which satisfy the following condition: $P^*\geqslant0$.

III. EXPERIMENTAL METHODS

A. Meso-PS fabrication

100 μm thick meso-PS layers were formed by means of well-known anodic dissolution process[19] that is usually achieved in HF-based electrolytes. In this work, monocrystalline (100)-oriented highly doped p^+-type Si wafers with resulting electrical resistivity of about 0.02 Ω cm and a standard electrochemical cell with metallic back-side electrode[19] were used. Due to the enhanced wafer doping concentration, ohmic contacts to the backside of the wafer were not necessary. Three PS circular samples with area of 1 cm^2 were fabricated in a solution of HF (50%) and ethanol [HF(50%): ethanol$\equiv$2:1] at different anodization current density values to ensure different porosity values of the porous samples. After fabrication, the samples were rinsed in deionized water. Then, the PS layers were oxidized in dry O_2 atmosphere for 1 h at different temperatures to ensure different oxidized fractions of the samples.

B. TC measurement by micro-Raman scattering

Using an Ar^+-ion laser with a wavelength of 514 nm focused on the PS samples, the micro-Raman backscattered spectra in parallel polarization were recorded by means of an Olympus BH2 microscope (objective $\times$50), coupled with a Dilor *XY* monochromator and a cooled photodiode array detector (Gold Dilor). The power distribution of the laser beam has a Gaussian nature.[20] However, a constant mean power value was assumed for the laser beam diameter of 5 μm.

To measure TC of the meso-PS layers, a measurement method already described in details[10] was applied. Heating laser beam focused on the PS sample generates a local temperature rise depending mainly on the local TC value. By measuring the Raman peak positions corresponding to two different heating power values (P_1 and P_2, $P_2 > P_1$), a simple linear model combining $\Delta P = P_2 - P_1$, $\Delta T = T_2 - T_1$ (T_1 and T_2 are the local temperatures corresponding to P_1 and P_2, respectively) and local TC of PS layer ($k_{\text{meso-PS}}$) can be used:

$$k_{\text{meso-PS}} = \frac{2\Delta P}{\pi a \Delta T}, \tag{12}$$

where a is the laser beam diameter. T_1 and T_2 have been determined by means of a calibration curve obtained at a low laser power provoking no heating of the sample and correlating the Raman peak position to bulk PS temperature.

C. Measurement of Si nanocrystallites mean size by micro-Raman scattering

This kind of measurement is already well documented in literature.[11–14] The nanocrystallite dimensions were estimated by means of the calibration curve calculated in Ref. 12 and correlating the Raman peak full width at half maximum to the Si nanocrystallites size. The Raman spectra were obtained at low laser power value when sample heating is negligible. The nanocrystallites are assumed to have a spherical form.[12]

D. Estimation of the meso-PS oxidized fraction

Chemical composition analysis made by means of energy dispersive x-ray fluorescence spectroscopy (EDXRFS) gives the ratio [O]/[Si] between oxygen (O) and silicon (Si) atoms constituting the oxidized meso-PS layer. When the layer is completely oxidized (100% oxidized fraction), i.e., when all Si atoms of the porous layer are bounded by O atoms to form SiO_2 molecules, the ratio $[O]/[Si] \approx 2$. Therefore, an oxidized fraction (ξ) of partially oxidized PS can be determined by the following relation:

$$\xi = \frac{1}{2} \frac{[O]}{[Si]} \times 100\%. \tag{13}$$

In our work, oxidized fractions corresponding to different oxidation temperatures have been determined on separate samples.

IV. RESULTS AND DISCUSSION

A. Surface TC of as-prepared meso-PS

First of all, the laser beam was focused on surfaces of the as-prepared PS layers formed at different anodization current densities (ACD). Si nanocrystallite sizes and TC of the layers were determined by the procedures described previously. As shown in Table I, TC of as-prepared meso-PS is considerably smaller than TC of monocrystalline Si ($k_{\text{Si}} = 150\,\text{W m}^{-1}\,\text{K}^{-1}$). In addition, the higher the ACD values forming the PS layers with higher porosity,[19] the lower the TC of the layers. These results can be illustrated by our
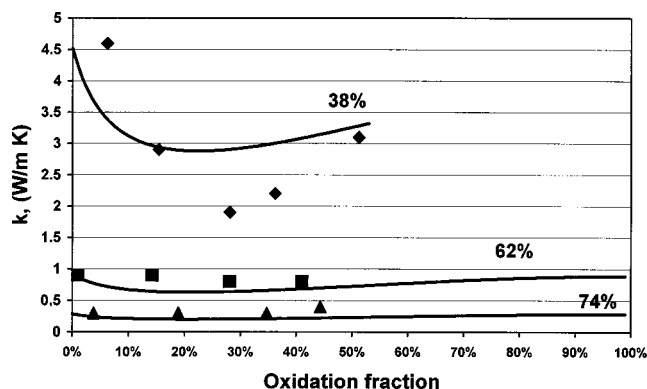

FIG. 4. Dependence of the TC of meso-PS on silicon oxidized fraction for three different porosity values. TC values measured by micro-Raman scattering: (◆) 38%, (■) 62%, (▲) 74%. The straight lines correspond to the theoretical model described by Eq. (11).

model. Indeed, according to Eq. (5), two facts: (1) $r_{\text{cr}} < \Lambda_{\text{Si}}$ and (2) $k_{\text{meso-PS}} \sim (1-P)^3$ can explain that $k_{\text{meso-PS}} \ll k_{\text{Si}}$ and that $k_{\text{meso-PS}}$ varies dramatically with the layer porosity. The similar conclusions have already been done for nano-PS.[2] Our measurement results are in good agreement with those made by means of thin films microdevices[2] and photoacoustic spectroscopy.[3]

Using Eq. (5) and the data of TC and Si nanocrystallite sizes measurements performed by micro-Raman spectroscopy, we have estimated local surface porosity of the PS layers whereas it is usually determined by gravimetric,[2,19] adsorption,[21] or by reflectivity measurements.[3]

B. Surface TC of partially oxidized meso-PS

The TC evolution with increasing meso-PS oxidized fraction (ξ) is presented in Fig. 4. The evolution dynamics predicted by Eq. (11) (straight line) for three different porosity values is in good agreement with measurements carried out by micro-Raman scattering. The oxidation influence on TC of high porous samples is negligible in comparison with the sample of 38% porosity. For the latter, the TC decreases in the range of small ξ values and has a minimum value at $\xi \approx 25\%$. It corresponds to heat transport preferably through the Si cores. Then, the TC increases with increasing oxidized fraction because of the heat transport occurring through the growing oxide sheet. For the samples with higher porosity, the theoretical function $k^*_{\text{meso-PS}} = f(\xi)$ have also a minimum but not so remarkable as for the small porosity sample. Experimental detection of this slight minimum needs higher measurement resolution of the experimental setup.

C. TC inhomogeneity along the meso-PS layer thickness

Nanostructure morphology in depth of the relatively thin meso-PS layers was already observed[22] to be changed in comparison with the surface one. According to our model, it can consequently lead to the corresponding TC changes, which will be especially important in thick ($\geqslant 100\,\mu m$) PS
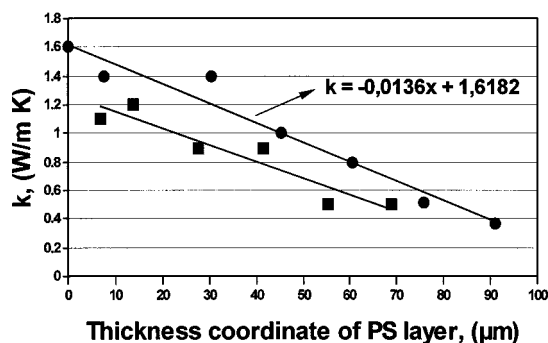
FIG. 5. TC inhomogeneity along meso-PS layers: (●) as-prepared layer (59% porosity), (■) porous layer oxidized at 300 °C in dry O_2 atmosphere for 1 h.

layers. Use of micro-Raman scattering allowed us to study the TC inhomogeneity along the meso-PS layer thickness of 100 μm.

Focusing the laser beam of 5 μm diameter on the cross section of the 100 μm thick PS samples of 59% porosity and scanning from the layer surface to its bottom, we measured TC gradient along the porous layer thickness. This kind of measurement cannot be performed by the usual techniques,[1–5] giving an average TC value of the whole PS layer. TC dependence on the layer thickness coordinate is shown in Fig. 5. The measurement corresponding to 0 μm was done on the layer surface. As it can be seen, TC of thick, both as-prepared and oxidized (at 300 °C in dry O_2 atmosphere for 1 h), PS layers does not remain constant along the layer thickness. Considerable TC decrease can be explained by variation of the layer morphology. To check it, Si nanocrystallite sizes were measured along the layer thickness. As the nanocrystallite sizes also decrease (Fig. 6), it provokes the decrease of the TC. Indeed, regarding Eq. (5), the smaller the nanocrystallite diameter (r_{cr}) is, the smaller the TC of meso-PS ($k_{meso-ps}$) is. Using the measured TC and nanocrystallite size gradients along the porous layer thickness and Eq. (5), a porosity gradient can be calculated (Fig. 6). As one can see, the porosity increases along the thickness.

Variations of the layer morphology (porosity and nanocrystallites size) can be explained by a decrease of HF concentration at the depth of the PS during the layer formation.[22] Indeed, because of reduced HF diffusion into the deeper
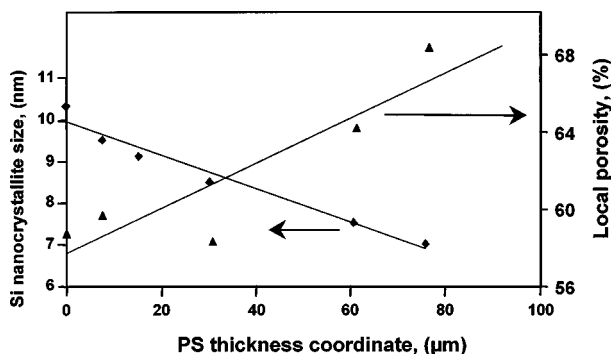
layer parts, the local acid concentration decreases and provokes formation of the deeper PS layer parts with enhanced porosity's[19,22] and reduced nanocrystallite diameters. Directly conditioning the heat transfer in PS [Eq. (5)], these morphological variations predetermine TC decrease along the layer thickness. For thermal isolation the TC decrease is a positive fact but from mechanical view point the corresponding porosity increase is not desirable.

This study shows that TC of the thick meso-PS layer's depends on the layers thickness. TC measurements only performed on the layer surface are not sufficient. To have a correct idea about TC of the whole porous layer, the measurements along the layer thickness have to be carried out. In general, an *apparent* TC value can be used to characterize thick meso-PS layers. Indeed, by assuming a linear dependence of TC on the layer thickness shown in Fig. 5 ($k_{meso-PS} = -0.0136x + 1.6$, where x is the thickness coordinate), the apparent TC of the whole PS layer ($\overline{k_{meso-PS}}$) can be calculated from mean value of thermal resistivity ($\overline{\rho_{meso-PS}}$) of the layer:

$$\overline{k_{meso-PS}} = \frac{1}{\overline{\rho_{meso-PS}}} = \frac{dA}{\ln\left(\dfrac{B}{B-dA}\right)}, \tag{14}$$

where A and B are the linear coefficients of the function $k_{meso-PS} = -0.0136x + 1.6$ and equal -0.0136×10^6 (W/m^2 K) and 1.6 (W/m K), respectively, and d is the layer thickness. In our case, $\overline{k_{meso-PS}} = 0.74$ (W/m K).

V. CONCLUSIONS

The theoretical model described in this article underlines the dependence of the TC of meso-PS layers on porosity, Si nanocrystallite diameters, and oxidation fraction. To obtain meso-PS with a given TC value, formation conditions and post-fabrication treatment of the layer have to be well controlled. The model is in good agreement with experimental results obtained by means of a recently described technique[10] for TC measurements based on micro-Raman scattering. Being simultaneously associated with size measurements of Si nanocrystallites and the theoretical model, this technique gives a new approach for estimation of local porosity of the porous samples. TC inhomogeneity along the meso-PS layer thickness was studied. From a practical point of view, an optimum between low TC and good mechanical stability of the thick meso-PS layers has to be found to apply them as a new thermal insulating substrate.

FIG. 6. Si nanocrystallite size (◆) and porosity (▲) variations along the PS layer thickness.

[1] A. Drost, P. Steiner, H. Moser, and W. Lang, Sens. Mater. **7**, 111 (1995).
[2] G. Gesele, J. Linsmeier, V. Drach, J. Fricke, and R. Arens-Fischer, J. Phys. D **30**, 2911 (1997).
[3] G. Benedetto, L. Boarino, and R. Spagnolo, Appl. Phys. A: Mater. Sci. Process. **64**, 155 (1997).
[4] G. Benedetto, L. Boarino, N. Brunetto, A. Rossi, R. Spagnolo, and G. Amato, Philos. Mag. B **76**, 383 (1997).
[5] N. Obraztsov, V. Yu. Timoshenko, H. Okushi, and H. Watanabe, Semiconductors **31**, 534 (1997).
[6] V. Lysenko, L. Boarino, M. Bertola, B. Remaki, A. Dittmar, G. Amato, and D. Barbier, Microelectr. J. **30**, 1141 (1999).

[7] W. Lang, P. Steiner, U. Schaber, and A. Richter, Sens. Actuators A **43**, 185 (1994).

[8] V. Lysenko, Ph. Roussel, G. Delhomme, V. Rossokhaty, V. Strikha, A. Dittmar, D. Barbier, N. Jaffrezic-Renault, and C. Martelet, Sens. Actuators A **67**, 205 (1998).

[9] Ph. Roussel, V. Lysenko, B. Remaki, G. Delhomme, A. Dittmar, and D. Barbier, Sens. Actuators A **74**, 100 (1999).

[10] S. Perichon, V. Lysenko, B. Remaki, B. Champagnon, and D. Barbier, J. Appl. Phys. **86**, 4700 (1999).

[11] H. Campbell and Ph. M. Fauchet, Solid State Commun. **58**, 739 (1986).

[12] Ph. M. Fauchet, in *Light Scattering in Semiconductor Structures and Superlattices*, edited by D. J. Lockwood and J. F. Young (Plenum, New York, 1991), p. 229.

[13] Z. Sui, P. P. Leong, I. P. Herman, G. S. Higashi, and H. Temkin, Appl. Phys. Lett. **60**, 2086 (1992).

[14] H. Münder, C. Andrzejak, M. G. Berger, U. Klemradt, H. Lüth, R. Herino, and M. Ligeon, Thin Solid Films **221**, 27 (1997).

[15] L. Smith and S. D. Collins, J. Appl. Phys. **71**, R1 (1992).

[16] M. I. J. Beale, J. D. Benjamin, M. J. Uren, N. G. Chew, and A. J. Cullis, J. Cryst. Growth **73**, 622 (1985).

[17] G. Chen, J. Heat Transfer **118**, 539 (1996).

[18] A. Majumdar, J. Heat Transfer **115**, 7 (1993).

[19] A. Halimaoui, in *Porous Silicon: Science and Technology*, edited by J.-C. Vial and J. Derrien (Springer, Berlin Heidelberg and Les Editions de Physique, Les Ulis, 1995), p. 33.

[20] M. Lax, J. Appl. Phys. **48**, 3919 (1977).

[21] R. Herino, G. Bomchil, K. Barla, C. Bertrand, and J. L. Ginoux, J. Electrochem. Soc. **134**, 1994 (1987).

[22] S. Billat, M. Thönissen, R. Arens-Fischer, M. G. Berger, M. Krüger, and H. Lüth, Thin Solid Films **297**, 22 (1997).